Epigallocatechin Gallate Induces Hepatic Stellate Cell Senescence and Attenuates Development of Hepatocellular Carcinoma

Mozhdeh Sojoodi[1], Lan Wei[1], Derek J. Erstad[1], Suguru Yamada[1], Tsutomu Fujii[1], Hadassa Hirschfield[2], Rosa S. Kim[2], Gregory Y. Lauwers[3], Michael Lanuti[4], Yujin Hoshida[2], Kenneth K. Tanabe[1], and Bryan C. Fuchs[1]

ABSTRACT

Hepatocellular carcinoma (HCC) is a highly morbid condition with lack of effective treatment options. HCC arises from chronically inflamed and damaged liver tissue; therefore, chemoprevention may be a useful strategy to reduce HCC incidence. Several reports suggest that epigallocatechin gallate (EGCG), extracted from green tea, can suppress liver inflammation and fibrosis in animal models, but its role in HCC chemoprevention is not well established. In this study, male Wistar rats were injected with diethylnitrosamine at 50 mg/kg for 18 weeks to induce cirrhosis and HCC, and EGCG was given in drinking water at a concentration of 0.02%. Clinically achievable dosing of EGCG was well-tolerated in diethylnitrosamine-injured rats and was associated with improved serum liver markers including alanine transaminase, aspartate transaminase, and total bilirubin, and reduced HCC tumor formation. Transcriptomic analysis of diethylnitrosamine-injured hepatic tissue was notable for increased expression of genes associated with the Hoshida high risk HCC gene signature, which was prevented with EGCG treatment. EGCG treatment also inhibited fibrosis progression, which was associated with inactivation of hepatic stellate cells and induction of the senescence-associated secretory phenotype. In conclusion, EGCG administered at clinically safe doses exhibited both chemopreventive and antifibrotic effects in a rat diethylnitrosamine liver injury model.

Introduction

Hepatocellular carcinoma (HCC) incidence has more than tripled since 1980, with 50,000 new cases predicted annually in the United States (1). HCC is a highly morbid condition with a 5-year survival less than 15%. Surgical resection, liver transplant, and radiofrequency ablation are considered the only curative therapies. However, the majority of patients are diagnosed at an advanced stage, and less than 20% of new cases are considered potentially curable. In addition, HCC is minimally responsive to standard chemotherapeutic agents (2). Until recently, sorafenib was the only drug clinically approved by FDA for treatment of advanced-stage HCC, even though sorafenib has been shown to provide only a modest survival benefit (3, 4).

Given the dismal outlook for HCC therapy, there has been increased interest in chemopreventive strategies. HCC arises from *a milieu* of chronically inflamed and damaged liver tissue, and thus there is a strong association between cirrhosis and HCC risk (5, 6). Typically, cirrhosis onset occurs years before a diagnosis of HCC, therefore, chemoprevention is highly applicable in this context given the large window of time for intervention.

Although HCC derives from hepatocytes, there is a strong association between liver fibrosis and HCC risk; therefore, stromal cells may play a role in mediating hepatocarcinogenesis (7–9). Hepatic stellate cells (HSC), the primary stromal cell type of the liver, transition to an "activated" myofibroblast-like state upon injury characterized by expression of smooth muscle actin and deposition of extracellular matrix components including collagens and matrix metalloproteinases (MMP). Persistent injury, as in the case of cirrhosis, may result in a state of chronic inflammation and tonic HSC activation, resulting in a pathologic fibrotic response (10). In addition, activated HSCs have also been shown to provide feed-forward stimuli by production of cytokines and chemokines that recruit inflammatory cells to the site of injury, raising concern that persistent HSC activation may support a protumorigenic environment (11). Accordingly, it has been predicted that direct inactivation of HSCs, or senescence, beneficially influences the dynamic balance of inflammation, fibrosis progression, and

[1]Division of Surgical Oncology, Massachusetts General Hospital Cancer Center and Harvard Medical School, Boston, Massachusetts. [2]Liver Tumor Translational Research Program, Harold C. Simmons Comprehensive Cancer Center, Division of Digestive and Liver Diseases, Department of Internal Medicine, University of Texas Southwestern Medical Center, Dallas, Texas. [3]Department of Pathology, Massachusetts General Hospital and Harvard Medical School, Boston, Massachusetts. [4]Division of Thoracic Surgery, Massachusetts General Hospital Cancer Center and Harvard Medical School, Boston, Massachusetts.

M. Sojoodi and L. Wei contributed equally to this article.

Corresponding Authors: Mozhdeh Sojoodi, Massachusetts General Hospital, 55 Fruit Street, W401, Boston, MA, 02138. Phone: 617-724-3839; Fax: 617-726-4442; E-mail: MSOJOODI@mgh.harvard.edu; and Bryan C. Fuchs, E-mail: BFUCHS@mgh.harvard.edu

Cancer Prev Res 2020;13:497–508

doi: 10.1158/1940-6207.CAPR-19-0383

HCC development, and may therefore provide a useful chemopreventive strategy (12).

Experimental and epidemiologic studies suggest tea polyphenols may have chemopreventive effects in variety of cancers including HCC (13, 14). Green tea is a rich source of natural polyphenols, which are commonly known as catechins, and epigallocatechin gallate (EGCG) is the most abundant catechin in green tea (comprising 50%–80% of the total pool). Several studies have reported the inhibitory effect of EGCG on cancer cell proliferation through inhibition of receptor tyrosine kinases and their downstream signaling pathways (15). EGCG has also been reported to induce cell-cycle arrest through expression of p21, p18, and p53, and inhibition of cyclins and cyclin-dependent kinases (15, 16). Finally, EGCG has been shown to reduce liver inflammation and fibrosis (17). Therefore, we hypothesized that EGCG would have chemopreventive effects in chronic liver injury through its negative regulation of inflammation, fibrosis, and cellular proliferation.

Materials and Methods

Animals

All animal experiments were approved by the Massachusetts General Hospital Institutional Animal Care and Use Committee. Animals were maintained on a 12-hour light/dark cycle at 25°C and fed a standard diet. To induce liver injury, cirrhosis, and HCC, rats were given weekly injections of low dose diethylnitrosamine (DEN; 50 mg/kg, i.p., Sigma-Aldrich) according to our established protocols (18–20). Diethylnitrosamine is a commonly used carcinogen for the liver, and the resultant tumors are known to genetically resemble human HCC tumors with poor prognosis (21, 22). We have also previously shown that diethylnitrosamine-induced liver injury has a similar progression to human disease, albeit on an accelerated course, first with the appearance of fibrosis at 8 weeks, then advanced fibrosis by 12 weeks, and marked liver cirrhosis with HCC at 18 weeks. Male Wistar rats (Charles River Laboratories) were given weekly intraperitoneal injections of 50 mg/kg of diethylnitrosamine for 18 weeks. A subset of rats received EGCG in their drinking water at concentration of 0.02% (0.02 g/100 mL) beginning at the 13th week when fibrosis is established but before the onset of HCC. Treatment was continued for 6 weeks until the study endpoint. On average, rats drink 50 mL of water per day, which means that the average rat in our study consumed 10 mg of EGCG per day. Because the average rat weighed 400 g, our relative dose in this study was approximately 25 mg/kg. Using the calculation, human equivalent dose (HED) (mg/kg) = animal dose (mg/kg) × (animal K_m/human K_m), we calculated the HED at 5.4 mg/kg. Assuming an average human weight of 80 kg, our dose would be approximately 432 mg per day.

Histologic analysis

Formal-fixed, paraffin embedded tissues samples were sectioned with 5 μm thicknesses and stained with hematoxylin and eosin, Masson trichrome, and antibodies for alpha-smooth muscle actin (α-SMA, ACTA2; 1:100, Sigma-Aldrich) and collagen, type 1, alpha 1 (COL1A1; 1:200, Abcam) according to standard protocols as reported previously (18). A board-certified pathologist scored the fibrosis according to the method of Ishak in a blinded manner.

Serum test

A cardiac terminal blood withdrawal was performed at the time of sacrifice. Blood was allowed to clot for 2 hours at room temperature before centrifugation at 2,000 rpm for 10 minutes at 4°C. Serum was isolated and stored at −80°C. Biochemical markers of liver injury were measured, including alkaline phosphatase (ALP), alanine transaminase (ALT), aspartate transaminase (AST), total bilirubin (TBIL), and albumin (DRI-CHEM 4000 Analyzer, Heska).

Western blot analysis

Liver tissue (0.01–0.05 g) was lysed with RIPA Buffer (Sigma-Aldrich) containing protease and phosphatase inhibitors. The isolated lysates were cleared by centrifugation and protein concentrations were measured with the BCA Protein Assay Kit (Thermo Fisher Scientific). Twenty milligram of total protein was separated by SDS-PAGE and transferred to a polyvinylidene difluoride membrane. Nonspecific binding was blocked by 10% skim milk in TBS supplemented with 0.1% Tween 20 (TBST). Immunoblots were performed using antibodies raised against α-SMA (1:2,000, Sigma-Aldrich) and β-actin (1:10,000, Abcam). Immune complexes were visualized by enhanced chemiluminescence (Pierce).

Senescence-associated β-galactosidase staining

Senescence-associated β-galactosidase (SA-β-gal) activity was measured by *in situ* staining using a chromogenic substrate under acidic conditions (23). Liver sections were rinsed twice in PBS and then incubated at 37°C in a freshly prepared X-gal solution containing 1 mg/mL X-gal (5-bromo-4-chloro-3-indolyl P3-D-galactoside; Sigma-Aldrich), 150 mmol/L sodium phosphate pH 6.0, 5 mmol/L potassium ferrocyanide, 5 mmol/L potassium ferricyanide, 50 mmol/L NaCl, and 2 mmol/L MgCl. Slides were incubated for 16 hours.

Cell culture

TWNT4 cells were cultured in DMEM supplemented with 100 μg/mL streptomycin, 100 units/mL penicillin, and 2 mmol/L L-glutamine (all from Cellgro) and 10% FBS (Atlanta Biologicals). Cells were maintained at 37°C in an atmosphere containing 5% CO_2 and 100% humidity. TWNT4 cells were seeded (10^4 cells/well) on a 24-well plate for 12 hours to attach. Cells were treated with increasing concentrations of EGCG. After 72 hours, 20-μL MTT solution (0.25 g/mL; Sigma-Aldrich) was added, and cells were incubated at 37°C for 4 hours. Another 100 μL of DMSO (Sigma-Aldrich) was added to each well to dissolve the purple formazon crystals after the removal of the MTT solution, and the plate was gently shaken at room temperature for 20 minutes. The optical density was measured at 570 nm using a Microplate Reader (Molecular Devices Emax).

RNA extraction and real-time PCR

Total RNA isolation, amplification, and normalization of data were done as described previously (18). Primer and probe sequences for qPCR were purchased from Applied Biosystems Inc.

Image acquisition and analysis

Images were captured with a Nikon Eclipse Microscope equipped with an Insight CMOS 5.1 digital camera. For quantification, at least 2,000 cells were counted per sample using the cell counter plugin in ImageJ.

Microarray and data analysis

Total RNA was extracted from liver tissue using TRizol (Invitrogen) according to the manufacturer's instructions and subsequently treated with DNase I (Promega). Genome-wide gene expression profiling was performed using RatRef-Expression BeadChip Microarrays (Illumina). Scanned data were normalized using cubic spline algorithm, summarized into official gene symbol, and mapped to human orthologous genes using the mapping table provided by the Jackson Laboratory (www.informatics.jax.org). Genes on the microarray were rank-ordered according to differential expression between the experimental conditions. Over- or underrepresentation of each gene signature on the rank-ordered gene list was evaluated on the basis of random permutation test. FDR < 0.25 was regarded as statistically significant. All microarray data analysis was performed using GenePattern Analysis Toolkit (www.genepattern.org) and R statistical computing language (https://www.r-project.org/).

Results

EGCG prevents HCC development in diethylnitrosamine-injured rats

EGCG treatment grossly limited the development of HCC nodules (diethylnitrosamine 18.75 ± 1.76 vs. DEN + EGCG 9.125 ± 1.922; $P < 0.001$; **Fig. 1A** and **B**), and was associated

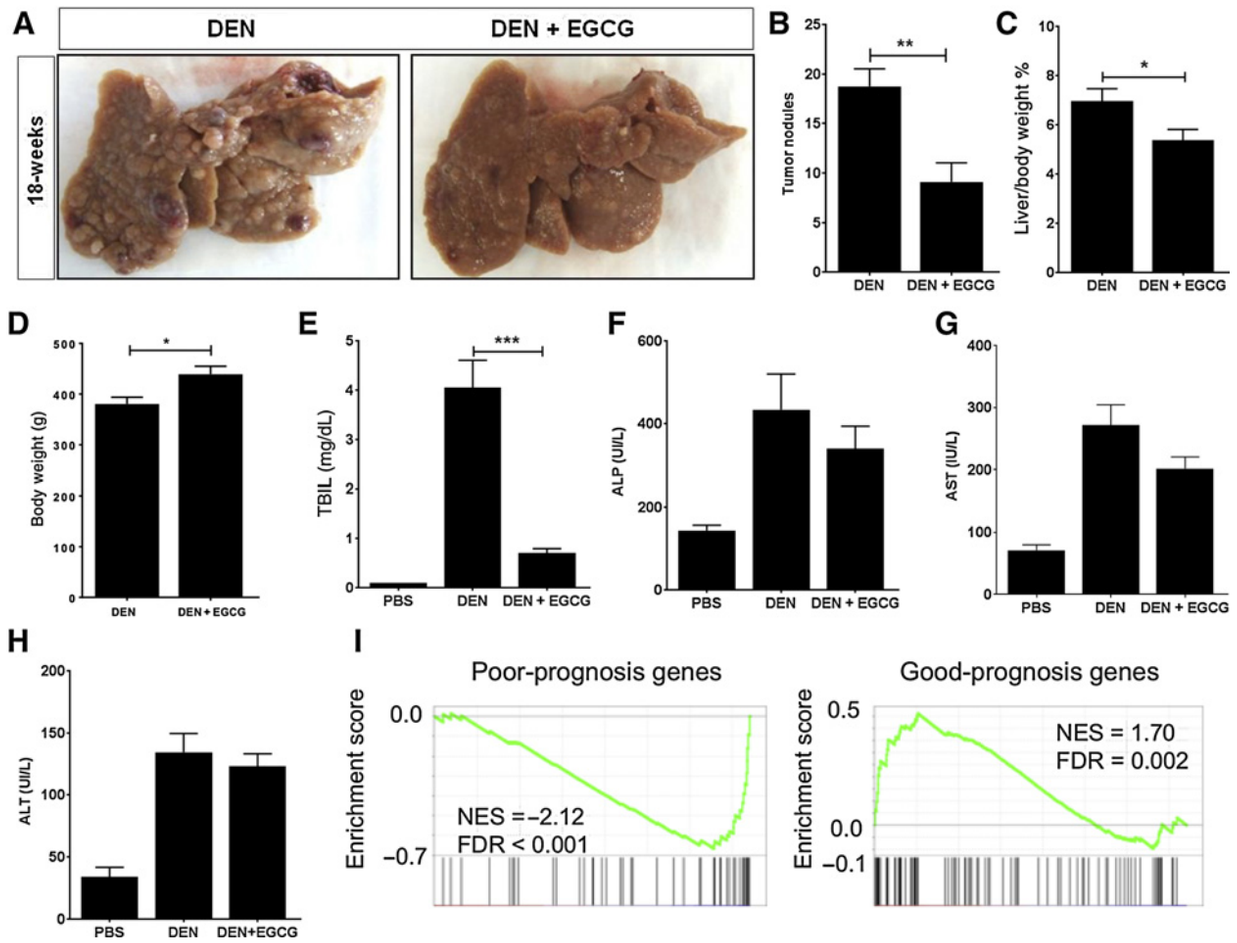

Figure 1.

EGCG inhibits HCC development in diethylnitrosamine (DEN)-injured rats. Male Wistar rats received weekly intraperitoneal injections of diethylnitrosamine for 18 weeks. After 12 weeks, a subset of rats received 0.02% EGCG in their drinking water during weeks 13–18. **A** and **B,** Representative rat liver images at the time of sacrifice. Tumors that were greater than 5 mm in diameter were counted. $N = 8$; **, $P < 0.01$ compared with untreated diethylnitrosamine controls. Liver/body weight (**C**) and body weight (**D**) was measured and compared with diethylnitrosamine-injured rats. *, $P < 0.05$. Serum levels of TBIL (**E**), ALP (**F**), AST (**G**), and ALT (**H**) are reported. $N = 4$ for all groups; ***, $P < 0.001$ compared with untreated diethylnitrosamine group. **I,** Gene set enrichment analysis of the 73-gene poor-prognosis signature and 113-gene good-prognosis signature in diethylnitrosamine-injured rats after treatment with EGCG.

with a significant reduction in the liver/body weight ratio (diethylnitrosamine 6.964% ± 0.5097% vs. DEN + EGCG 5.377% ± 0.4375%; $P < 0.05$; **Fig. 1C**). EGCG was well-tolerated and mitigated diethylnitrosamine toxicity–related weight loss (diethylnitrosamine 380.5 ± 13.23 g vs. DEN+EGCG 439.2 ± 15.79 g; $P < 0.05$; **Fig. 1D**). Commensurate with these gross findings, EGCG treatment also improved biochemical markers of liver function and injury, including TBIL, ALP, AST, and ALT, which were all decreased (**Fig. 1E–H**).

To better understand the mechanism of EGCG-mediated HCC chemoprevention, we performed transcriptomic analysis of nontumoral, hepatic tissue from diethylnitrosamine controls and EGCG-treated rats. Hoshida and colleagues previously reported a 186-gene signature derived from cirrhotic liver tissue that can discriminate patients by future HCC risk (24, 25). Diethylnitrosamine treatment resulted in transcriptomic changes that mirror Hoshida's poor prognosis signature. In contrast, EGCG treatment resulted in prevention of this signature toward a "good prognosis" expression profile (**Fig. 1I**). The significantly upregulated and downregulated gene clusters in EGCG-treated rats are shown in **Table 1**. Good prognosis genes enriched in EGCG-treated animals involve networks that participate in normal liver function such as organic acid

Table 1. Gene ontology (GO) functional enrichment analysis for up- and downregulated genes after treatment with EGCG.

No.	GO accession	Upregulated	NES	FDR	*P*
1	GO:0006082	Organic acid metabolic process	2.45	0	0
2	GO:0019752	Carboxylic acid metabolic process	2.36	0	0
3	GO:0032787	Monocarboxylic acid metabolic process	2.24	0	0
4	GO:0006631	Fatty acid metabolic process	2.15	0	0
5	GO:2001289	Lipid metabolic process	2.08	0	0.001
6	GO:0008654	Phospholipid biosynthetic process	1.98	0	0.002
7	GO:0044255	Cellular lipid metabolic process	1.97	0	0.003
8	GO:0016042	Lipid catabolic process	1.85	0.002	0.019
9	GO:0006732	Coenzyme metabolic process	1.85	0	0.018
10	GO:0044242	Cellular lipid catabolic process	1.84	0.005	0.017
11	GO:0046467	Membrane lipid biosynthetic process	1.83	0.004	0.018
12	GO:0008610	Lipid biosynthetic process	1.77	0	0.033
13	GO:0015980	Energy derivation by oxidation of organic compounds	1.77	0.005	0.032
14	GO:0044270	Nitrogen compound catabolic process	1.75	0.007	0.033
15	GO:0008202	Steroid metabolic process	1.73	0.002	0.038
16	GO:0006519	Amino acid and derivative metabolic process	1.72	0.002	0.043
17	GO:0006807	Nitrogen compound metabolic process	1.71	0	0.042
18	GO:0009056	Catabolic process	1.71	0	0.04
19	GO:0044248	Cellular catabolic process	1.65	0	0.065
20	GO:0006520	Amino acid metabolic process	1.64	0.015	0.067

No.	GO accession	Downregulated	NES	FDR	*P*
1	GO:0007599	Hemostasis	−1.91	0	0.063
2	GO:0030155	Regulation of cell adhesion	−1.87	0	0.056
3	GO:0007596	Blood coagulation	−1.83	0.004	0.073
4	GO:0009611	Response to wounding	−1.83	0	0.058
5	GO:0050817	Coagulation	−1.82	0.002	0.052
6	GO:0045597	Positive regulation of cell differentiation	−1.81	0.004	0.051
7	GO:0050878	Regulation of body fluid levels	−1.81	0.002	0.045
8	GO:0009605	Response to external stimulus	−1.73	0	0.1
9	GO:0051707	Response to other organism	−1.72	0	0.1
10	GO:0006952	Defense response	−1.71	0	0.102
11	GO:0042060	Wound healing	−1.7	0.002	0.103
12	GO:0008544	Epidermis development	−1.68	0.003	0.118
13	GO:0009617	Response to bacterium	−1.68	0.015	0.111
14	GO:0009607	Response to biotic stimulus	−1.67	0.005	0.117
15	GO:0045595	Regulation of cell differentiation	−1.67	0.002	0.11
16	GO:0051259	Protein oligomerization	−1.66	0.012	0.113
17	GO:0007398	Ectoderm development	−1.65	0.012	0.12
18	GO:0009888	Tissue development	−1.61	0.003	0.157
19	GO:0016337	Cell–cell adhesion	−1.61	0.009	0.156
20	GO:0050863	Regulation of t cell activation	−1.59	0.017	0.169

Note: Gene sets with FDR < 0.25 are shown (top 20 when there are >20 gene sets with FDR < 0.25).
Abbreviation: NES, normalized enrichment score.

metabolism, lipid and fatty acid metabolism and biosynthesis, amino acid metabolism, catabolic processes, and cellular catabolism. In contrast, the poor prognosis gene networks induced by diethylnitrosamine treatment are primarily involved in wound healing and fibrosis progression, including pathways related to cell adhesion, defense mechanisms, and coagulation. Importantly, these networks were significantly downregulated after EGCG treatment.

EGCG prevents cirrhosis progression in diethylnitrosamine-injured rats

EGCG treatment has previously been shown to have antifibrotic properties in rodent models of liver injury. In our study, EGCG treatment for 6 weeks was associated with decreased progression to cirrhosis, evidenced by reduced type I collagen staining in liver tissue (EGCG 2.64 ± 0.40 vs. diethylnitrosamine 15.78 ± 1.326; $P < 0.001$; **Fig. 2A** and **B**). Pathologic scoring of fibrosis using Masson trichrome staining also demonstrated significant improvement in the median Ishak score in EGCG-treated rats compared with untreated diethylnitrosamine controls [4.4, interquartile range (IQR) 2–6 compared with 5.8, IQR 5–6; $P < 0.05$; **Fig. 2C** and **D**].

EGCG promotes HSC senescence *in vivo*

Upon diethylnitrosamine injury, quiescent HSCs transform to activated α-SMA–positive myofibroblasts that proliferate and promote fibrogenesis. Diethylnitrosamine-injured rats that received 0.02% EGCG in their drinking water had significant reductions in immunostaining of α-SMA on paraffin-embedded liver samples compared with diethylnitrosamine controls, suggesting decreased HSC activation (**Fig. 3A** and **B**). This observation was corroborated by Western blot analysis, in which we again observed less α-SMA protein expression in livers isolated from EGCG-treated animals (**Fig. 3C**). Given the decrease in stromal activation, we investigated whether EGCG induced HSC senescence by measuring HSC SA-β-gal activity (26–28). SA-β-gal activity was increased in EGCG-treated liver tissue as compared with untreated diethylnitrosamine controls, indicating higher levels of senescence (**Fig. 3D** and **E**). SA-β-gal–positive cells were specifically located in the fibrotic bands where HSCs are abundant, but not in the surrounding hepatic tissue (**Fig. 3D**), indicating that EGCG induced senescence in HSCs but not hepatocytes. In addition, proliferating cell nuclear antigen (PCNA), a marker for cellular proliferation, was significantly decreased in EGCG-treated livers compared with untreated diethylnitrosamine controls (**Fig. 3F**).

A gene signature for activated HSCs was previously established and verified across multiple human datasets and animal models (29, 30). We performed microarray analysis of liver tissue from diethylnitrosamine and DEN+EGCG-treated animals and compared expression profiles with the activated HSC signature. EGCG treatment was associated with HSC inactivation, evidenced by loss of overlap with the

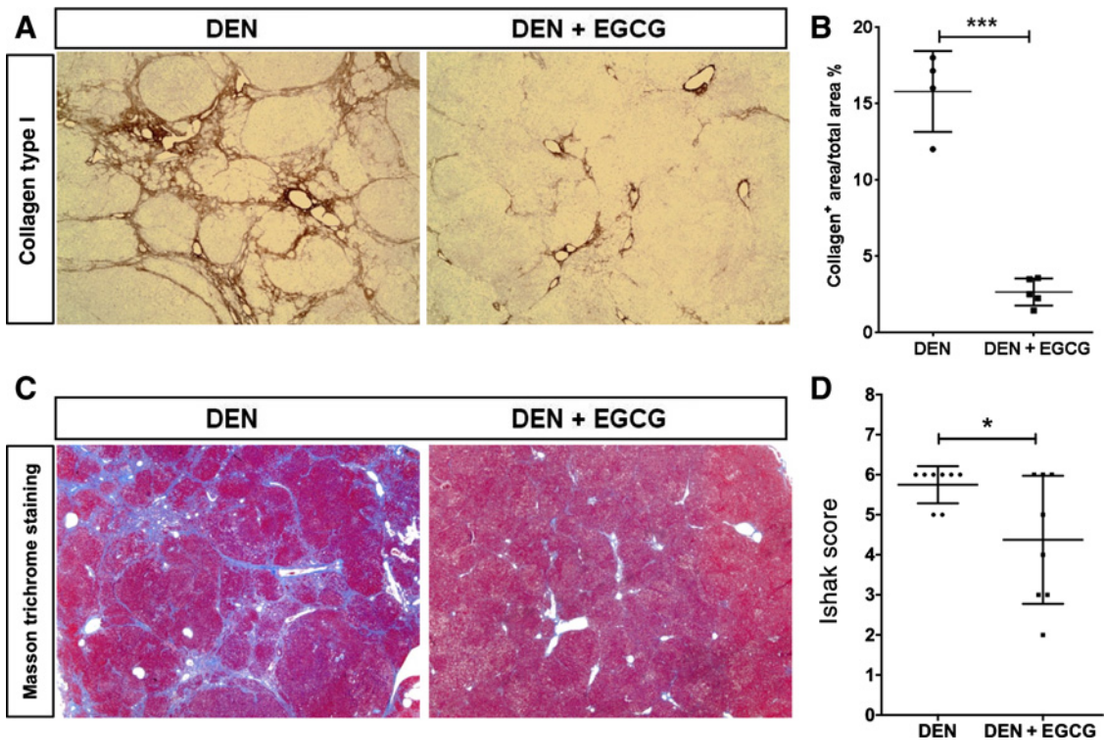

Figure 2.

EGCG decreases fibrosis progression to cirrhosis. **A** and **B,** Immunostaining for collagen I (magnification, 100×) was quantified. **C** and **D,** Masson trichrome stains of liver sections from each animal were scored by the method of Ishak. *, $P < 0.05$; ***, $P < 0.001$, compared with untreated diethylnitrosamine (DEN) group.

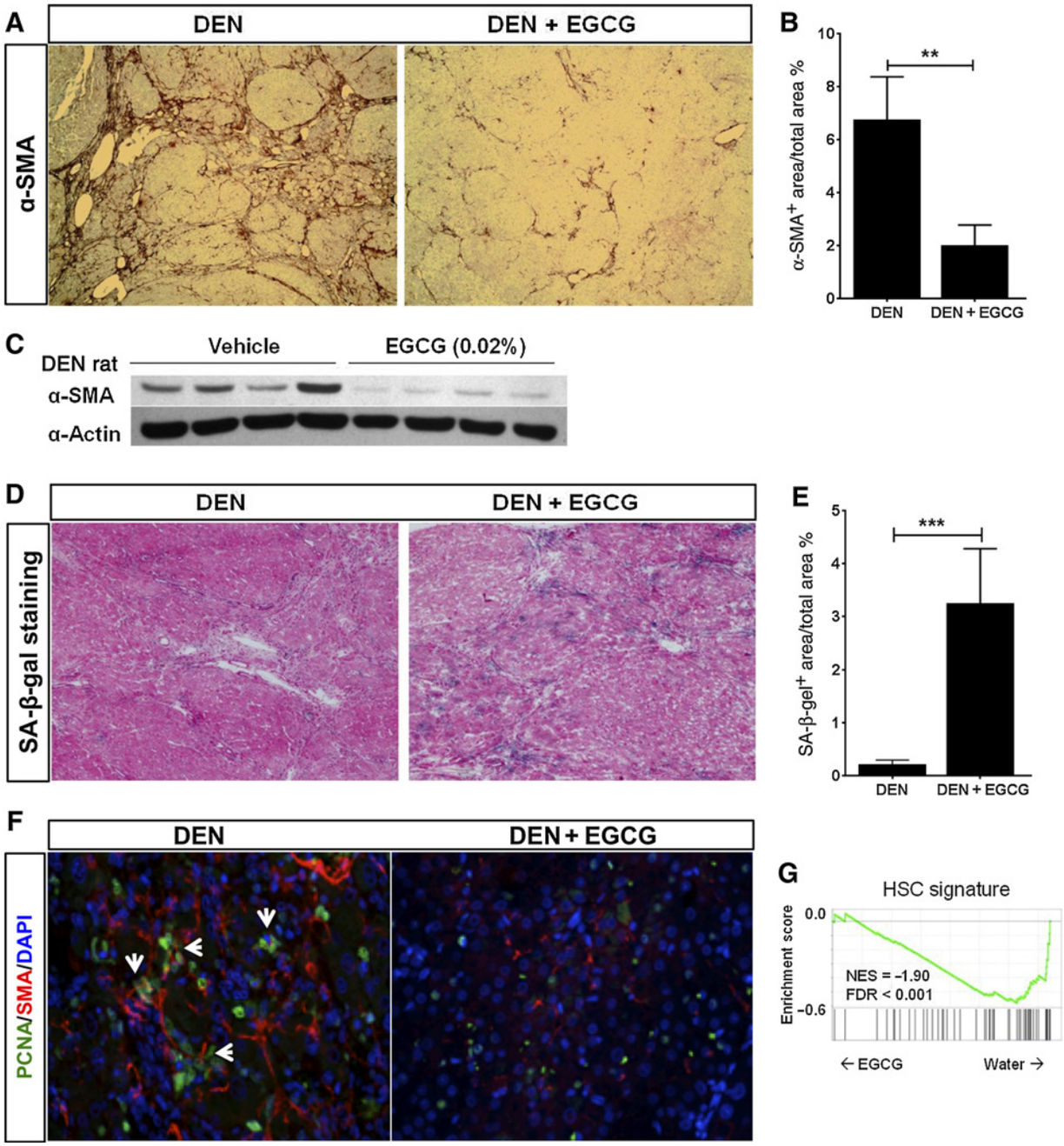

Figure 3.

EGCG induces cellular senescence of activated HSCs. **A** and **B,** Immunostaining of α-SMA (magnification, 100×) was quantified. **, $P < 0.01$. **C,** Representative Western blot analysis for α-SMA performed on nontumoral surrounding liver tissue lysates. **D** and **E,** SA-β-gal staining (turquoise blue) of liver sections of untreated and EGCG-treated diethylnitrosamine (DEN) animals was quantified. ***, $P < 0.001$. **F,** IHF staining for PCNA (green) and smooth muscle actin (SMA; red) on liver tissue from untreated and EGCG-treated diethylnitrosamine animals. **G,** Expression of HSC activation was assessed with a HSC gene signature in diethylnitrosamine-injured rats treated with vehicle (water) or EGCG.

HSC activation signature compared with untreated diethylnitrosamine controls (**Fig. 3G**). Taken together, these findings suggest that EGCG both reduced HSC activation and induced senescence in the setting of diethylnitrosamine liver injury.

EGCG promotes HSC senescence and senescence-associated secretory phenotype in HSCs *in vitro*

To gain more insight into EGCG-induced HSC senescence, we treated TWNT4 immortalized human HSCs *in vitro* with EGCG. EGCG treatment at concentrations above 20 μmol/L

significantly reduced cell proliferation compared with untreated controls by MTT assay. This growth reduction did not appear to be a toxic effect, as cells remained viable in the EGCG treatment groups on microscopic evaluation (**Fig. 4A** and **B**). Other general hallmarks of senescence include the absence of proliferative markers such as Ki67, and increased expression of tumor suppressors (P53) and cell-cycle inhibitors (P16 and P21). Consistent with these observations, 20 μmol/L EGCG treatment was also associated with significant reduction (≈1.5-fold) in Ki67 expression (control 48.59% ± 2.523% vs. EGCG 31.24% ± 2.039%; $P < 0.001$; **Fig. 4C** and **D**), and significant increases in cell-cycle inhibitor gene expression, including *P16, P21*, and *P53* (**Fig. 4G**). Finally, SA-β-gal activity also increased (≈4-fold) in TWNT4 cells after 72 hours of treatment with 20 μmol/L EGCG (control 22.52 ± 1.126 vs. EGCG 62.64 ± 1.255; $P < 0.001$; **Fig. 4E** and **F**). These findings corroborate our *in vivo* observation that EGCG induces HSC senescence.

Finally, previous reports have identified the presence of a unique secretory phenotype specifically associated with senescence in HSCs, which is characterized by reduced expression of extracellular matrix (ECM) proteins, increased expression of ECM-degrading enzymes, and increased secretion of inflammatory cytokines, referred to as the senescence-associated secretory phenotype (SASP; ref. 31). In our study, compared with untreated cells, EGCG-treated TWNT4 cells exhibited a similar secretory profile upon undergoing senescence *in vitro*, including: reduced expression of collagen type 1 (*COL1A1*), collagen type 3 (*COL3A1*), and fibronectin (*FN*; **Fig. 4H**); increased expression of MMP-1 (*MMP1*) and -3 (*MMP3*); and increased expression of immune surveillance chemokines, IL6 (*IL6*) and -8 (*IL8*; **Fig. 4I** and **J**). These findings therefore suggest that EGCG-induced senescence in HSCs also leads to initiation of SASP.

EGCG does not promote senescence of human HCC cell lines

To further demonstrate that EGCG-induced senescence is specific to HSCs, we treated the human HCC cell lines HepG2 and Hep3B with 20 μmol/L EGCG for 72 hours. EGCG treatment had no effect on SA-β-gal activity in HepG2 cells under normal growth conditions (vehicle 1.512% ± 0.19% vs. EGCG 1.231% ± 0.20%; **Fig. 5A** and **B**). In addition, no difference in senescence-associated gene expression was observed (**Fig. 5C**). Similarly, although Hep3B cells have more SA-β-gal activity (<15%) at baseline; no difference was observed with EGCG treatment (**Fig. 5D** and **E**). Finally, we did not observe any change in gene expression of the tumor suppressors, *P16* or *P21*, after EGCG treatment (**Fig. 5F**).

Discussion

Prior studies have shown a protective effect of the main constituent of green tea, EGCG, against liver injury, oxidative stress, inflammation, and fibrosis in experimental animal models of liver diseases (32–35). In this study, we recapitulate the observed antifibrotic effect in a diethylnitrosamine liver injury model and provide a novel mechanism through stellate cell-specific senescence. In addition, we report that EGCG treatment is also chemopreventive for the development of HCC after diethylnitrosamine injury.

Prior studies evaluating the hepatoprotective effects of EGCG often relied on high drug doses that have not been shown to be safe in humans. High doses of EGCG are hepatotoxic in mice (36), and at least 200 cases of EGCG-related hepatic toxicity have been reported since 1996, likely due to growing consumer interest in herbal supplements in the United States (36, 37). In contrast, the EGCG dose used in this study was designed to be equivalent to a human oral dose of 400 mg per day, which had been demonstrated to be safe and tolerable in a human single-dose ascending study (38). More recent results in humans have demonstrated elevations of ALT and AST after 12 months of green tea extract consumption (1,315 ± 115 mg total catechins including 843 ± 44 mg of EGCG per day) in a placebo-controlled, double-blinded phase II clinical trial assessing breast cancer risk biomarkers in healthy postmenopausal women (39). These elevations occurred in a small proportion of participants and were reversible. Therefore, we believe our results represent the first report showing clinically achievable and safe doses of EGCG can prevent fibrosis progression and prevent HCC development.

Multiple previous studies have demonstrated an association between hepatic fibrosis and HCC risk (18, 40, 41). Although the etiologies of liver disease have specific risks for development of HCC, most patients sequentially develop hepatitis, fibrosis, cirrhosis, and then HCC (42). In 80%–90% of patients, HCCs develops in fibrotic or cirrhotic environment and patients with a high serologic fibrosis index (FIB-4) have an up to 15-fold increased risk for future HCC incidence (43). In addition, one-third of patients with cirrhosis develop HCC within 5 years (42). Fibrogenesis in liver is mediated by HSCs, which deposit ECM molecules and recruit immune cells to the site of injury (44, 45). We previously reported that HSC inactivation prevents fibrosis progression, which is associated with a reduction in HCC development in rodents (18, 46). In this study, EGCG reduced fibrosis progression through induction of senescence in HSCs, which resulted in improved liver function and reduced HCC development

It has previously been shown that senescent HSCs develop a unique secretory phenotype known as the SASP. We observed a similar phenotype in HSCs *in vivo* and TWNT4 cells *in vitro* with EGCG treatment, which resulted in reduced proliferation as measured by Ki67 staining and MTT assay, and increased expression of senescence markers including increased SA-β-gal staining, and upregulation of tumor suppressor genes including *P16, P21*, and *P53*. TWNT4 cells also increase the expression of immunosurveillance cytokines (*IL6* and *IL8*), which are known to induce recruitment of natural killer cells, regulatory T lymphocytes, and macrophages to remove matrix debris and activated HSC (45, 47).

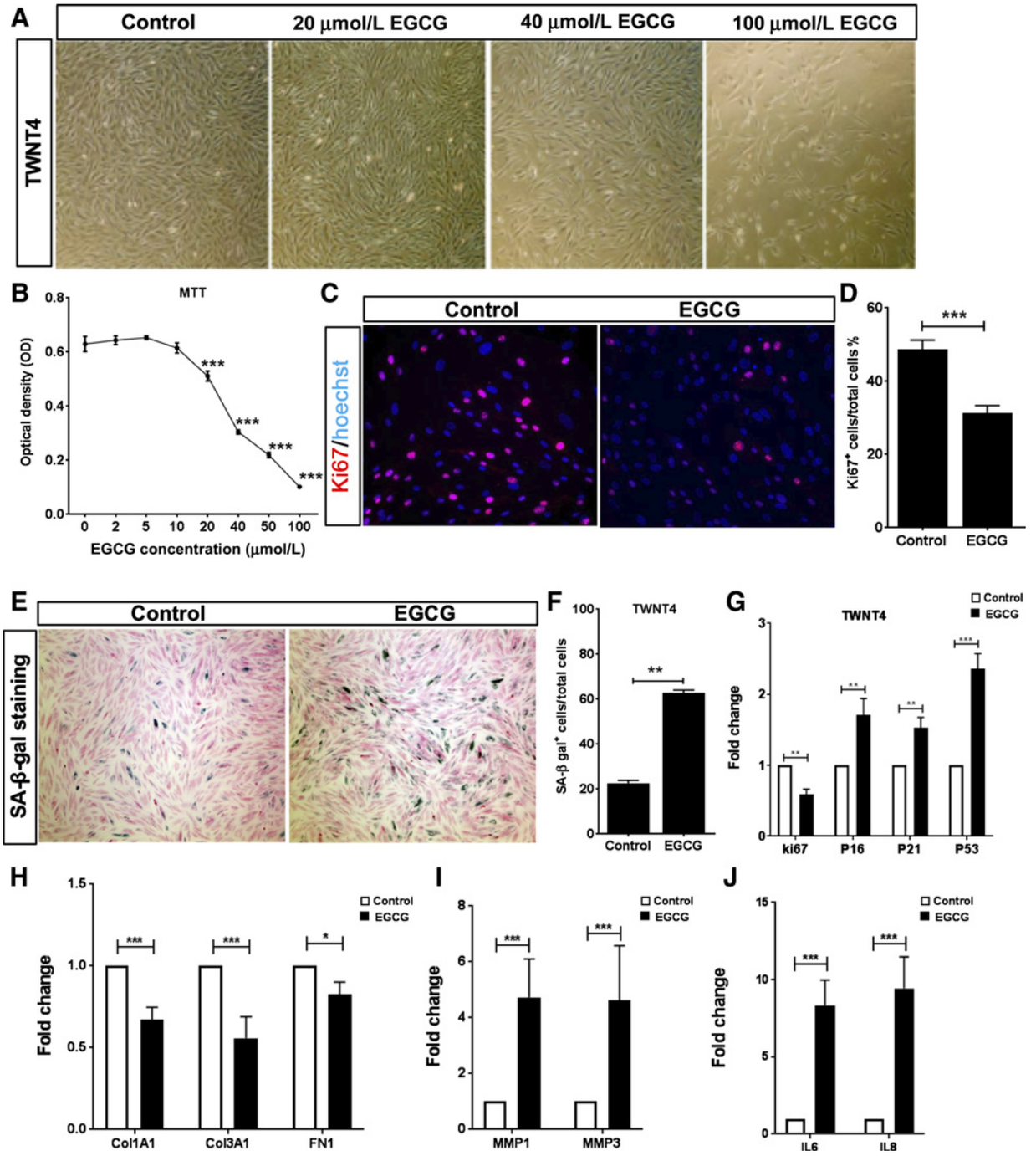

Figure 4.

EGCG induces SASP in human HSCs cell line *in vitro*. TWNT4 cells were treated with different concentration of EGCG (0, 2, 5, 10, 20, 40, 50, and 100 μmol/L) for 72 hours. **A,** Representative bright field pictures of TWNT4 cells treated with 20, 50, and 100 μmol/L of EGCG. **B,** MTT cell proliferation assay in TWNT4 cells, 72 hours after treatment with EGCG. **C** and **D,** Immunofluorescence staining of Ki67 (red) and DAPI (blue) on TWNT4 cells after 72 hours treatment with 20 μmol/L EGCG. Untreated cells were considered as control, 2,000 cells were counted in each group; ***, $P < 0.001$ compared with control. **E** and **F,** SA-β-gal staining (turquoise blue) of TWNT4 cells after 72 hours treatment with 20 μmol/L EGCG. Untreated cells were considered as control, 2,000 cells were counted in each group; **, $P < 0.01$ compared with control. **G–J,** RNA expression of senescence and SASP markers in TWNT4 cells after 72 hours treatment with 20 μmol/L EGCG. Untreated cells were considered as control. $N = 4$ replicates (*, $P < 0.05$; **, $P < 0.01$; ***, $P < 0.001$).

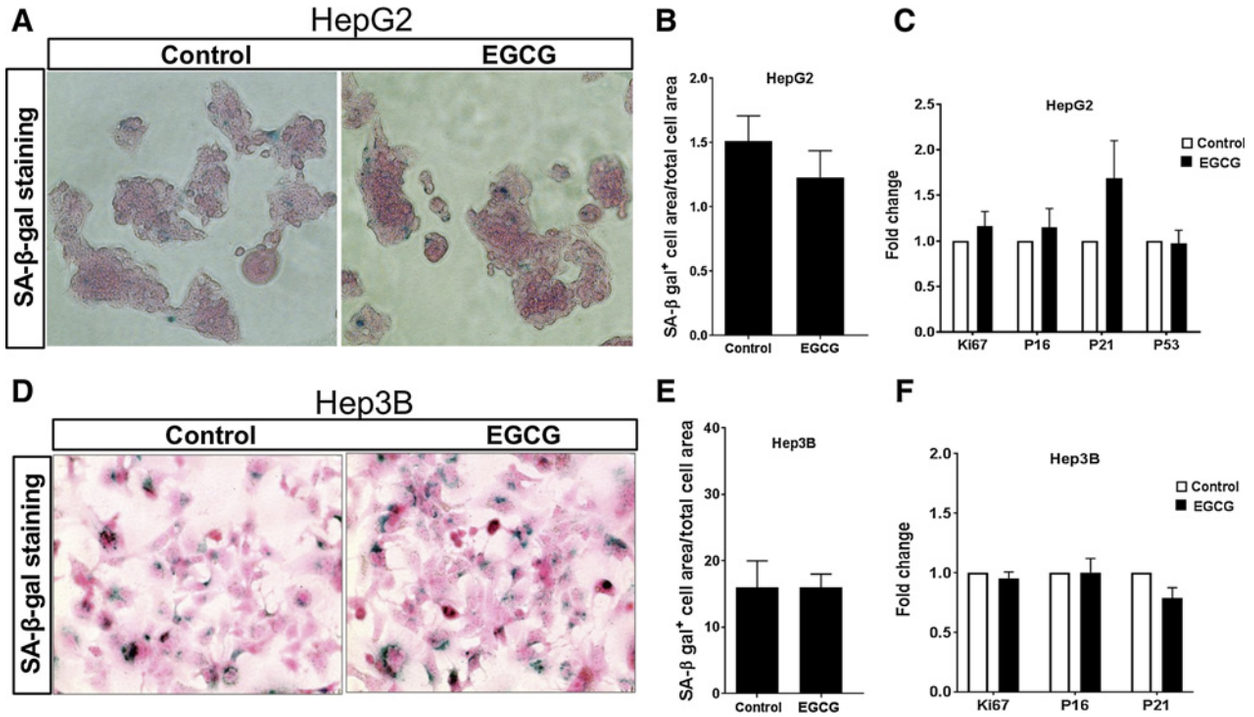

Figure 5.

EGCG does not alter senescence markers in human HCC cell lines *in vitro*. HepG2 and Hep3B cells were treated with 20 μmol/L of EGCG for 72 hours. **A** and **B,** SA-β-gal staining (turquoise blue) of HepG2 cells. A total of 2,000 cells were counted in each group. **C,** Expression of cell-cycle–associated genes in untreated and EGCG-treated HepG2 cells. **D** and **E,** SA-β-gal staining (turquoise blue) of Hep3B cells. A total of 2,000 cells were counted in each group. **F,** Expression of cell-cycle–associated genes in untreated and EGCG-treated Hep3B cells.

Interestingly, other reports have shown that the increased SASP from senescent HSC can induce HCC development (48, 49). These studies concluded that while cellular senescence usually provides a barrier to epithelial transformation, senescence in mesenchymal cells, like HSCs, could support cancer growth through the SASP by releasing cytokines like IL6. Most of these studies were performed in the context of obesity-associated HCC in animal models without significant fibrosis. The discrepancy in these studies could be explained by differences in the senescence triggers, the composition of microenvironment, and extent of senescence surveillance in different animal models (48, 50).

Other possible mechanisms could explain the reduction of HCC development after EGCG treatment. This includes reversibility of mutation load that is caused by diethylnitrosamine. In a high-fat diet (HFD) mouse model of HCC, theaphenon E, a standardized green tea extract formulation, blocked HCC formation via prevention of lipid peroxidation–derived mutagenic cyclic DNA-adduct (γ-OHPdG) formation resulting in decreased mutation load particularly G>T, the most common mutation in human HCC (51). Consistent with these results, theaphenon E reduced HCC incidence in xeroderma pigmentosum group A–knockout mice and diethylnitrosamine-injected mice and the reduction in HCC incidence was associated with decreased (γ-OHPdG) levels (52). In addition, using a microarray approach we showed that after EGCG treatment the pathways/genes involved in normal liver metabolic functions such as amino acid and lipid metabolism were markedly upregulated, and at the same time, pathways that are involved in wound healing and immune system response were downregulated. These mechanisms will need to be further evaluated in future studies.

Our data therefore suggests that the cancer prevention effects of EGCG-induced fibrosis regression, including the upregulation of ECM remodeling and inflammatory cytokines that contribute to the clearance of senescent cells and resolution of fibrotic tissue, outweigh any procancer effects of the SASP at least in the setting of cirrhosis. It is also possible that the SASP response needs to be combined with appropriate environmental cofactors, like DCA, which is produced by the gut microbiota in HFD and required for HCC development (48).

Green tea is very popular and mainly consumed in Asia. Several meta-analyses have been performed on Asian populations to investigate the association between green tea consumption and the risk for liver cancer (53–55). While some of these studies have shown no association with cancer risk (56), others have shown a decreased risk of liver cancer with green

tea consumption especially in people who drink more green tea for longer periods of time (54–56). Given the slow progression of cirrhosis to HCC development, green tea consumption represents a potentially safe and cheap chemopreventive strategy for HCC.

Disclosure of Potential Conflicts of Interest

K.K. Tanabe reports a patent to Prevention of fibrosis and hepatocellular carcinoma issued and research support from Enanta Pharmaceuticals and Zafgen to study drugs to prevent HCC. B.C. Fuchs reports receiving grants from American Institute for Cancer Research during the conduct of the study; grants from Blade Therapeutics, Collagen Medical, and Enanta Pharmaceuticals, and personal fees from Gilead Sciences and Ferring Pharmaceuticals outside the submitted work. No potential conflicts of interest were disclosed by the other authors.

Authors' Contributions

Conception and design: M. Sojoodi, L. Wei, D.J. Erstad, M. Lanuti, K.K. Tanabe, B.C. Fuchs
Development of methodology: M. Sojoodi, L. Wei, K.K. Tanabe, B.C. Fuchs
Acquisition of data (provided animals, acquired and managed patients, provided facilities, etc.): M. Sojoodi, L. Wei, S. Yamada, T. Fujii, R.S. Kim, G.Y. Lauwers, Y. Hoshida, B.C. Fuchs
Analysis and interpretation of data (e.g., statistical analysis, biostatistics, computational analysis): M. Sojoodi, L. Wei, D.J. Erstad, H. Hirschfield, R.S. Kim, Y. Hoshida, K.K. Tanabe, B.C. Fuchs
Writing, review, and/or revision of the manuscript: M. Sojoodi, L. Wei, D.J. Erstad, T. Fujii, Y. Hoshida, K.K. Tanabe, B.C. Fuchs
Administrative, technical, or material support (i.e., reporting or organizing data, constructing databases): L. Wei, T. Fujii, H. Hirschfield, K.K. Tanabe, B.C. Fuchs
Study supervision: K.K. Tanabe, B.C. Fuchs

Acknowledgments

This work was supported by an Investigator-Initiated Grant from the American Institute for Cancer Research (to B.C. Fuchs).

The costs of publication of this article were defrayed in part by the payment of page charges. This article must therefore be hereby marked *advertisement* in accordance with 18 U.S.C. Section 1734 solely to indicate this fact.

Received October 23, 2019; revised January 2, 2020; accepted March 31, 2020; published first April 6, 2020.

References

1. El-Serag HB, Kanwal F. Epidemiology of hepatocellular carcinoma in the United States: where are we? Where do we go? Hepatology 2014;60:1767–75.
2. Tsochatzis EA, Meyer T, Burroughs AK. Hepatocellular carcinoma. N Engl J Med 2012;366:92.
3. Kudo M, Lencioni R, Marrero JA, Venook AP, Bronowicki JP, Chen XP, et al. Regional differences in sorafenib-treated patients with hepatocellular carcinoma: GIDEON observational study. Liver Int 2016;36:1196–205.
4. Al-Rajabi R, Patel S, Ketchum NS, Jaime NA, Lu TW, Pollock BH, et al. Comparative dosing and efficacy of sorafenib in hepatocellular cancer patients with varying liver dysfunction. J Gastrointest Oncol 2015;6:259–67.
5. Sanyal AJ, Yoon SK, Lencioni R. The etiology of hepatocellular carcinoma and consequences for treatment. Oncologist 2010;15:14–22.
6. Fattovich G, Stroffolini T, Zagni I, Donato F. Hepatocellular carcinoma in cirrhosis: incidence and risk factors. Gastroenterology 2004;127:S35–50.
7. Tlsty TD. Stromal cells can contribute oncogenic signals. Semin Cancer Biol 2001;11:97–104.
8. Bhowmick NA, Neilson EG, Moses HL. Stromal fibroblasts in cancer initiation and progression. Nature 2004;432:332–7.
9. Geng ZM, Li QH, Li WZ, Zheng JB, Shah V. Activated human hepatic stellate cells promote growth of human hepatocellular carcinoma in a subcutaneous xenograft nude mouse model. Cell Biochem Biophys 2014;70:337–47.
10. Seki E, Schwabe RF. Hepatic inflammation and fibrosis: functional links and key pathways. Hepatology 2015;61:1066–79.
11. Tanaka H, Leung PS, Kenny TP, Gershwin ME, Bowlus CL. Immunological orchestration of liver fibrosis. Clin Rev Allergy Immunol 2012;43:220–9.
12. Coulouarn C, Clement B. Stellate cells and the development of liver cancer: therapeutic potential of targeting the stroma. J Hepatol 2014;60:1306–9.
13. Darvesh AS, Bishayee A. Chemopreventive and therapeutic potential of tea polyphenols in hepatocellular cancer. Nutr Cancer 2013;65:329–44.
14. Shimizu M, Shirakami Y, Sakai H, Kubota M, Kochi T, Ideta T, et al. Chemopreventive potential of green tea catechins in hepatocellular carcinoma. Int J Mol Sci 2015;16:6124–39.
15. Sah JF, Balasubramanian S, Eckert RL, Rorke EA. Epigallocatechin-3-gallate inhibits epidermal growth factor receptor signaling pathway. Evidence for direct inhibition of ERK1/2 and AKT kinases. J Biol Chem 2004;279:12755–62.
16. Masuda M, Suzui M, Weinstein IB. Effects of epigallocatechin-3-gallate on growth, epidermal growth factor receptor signaling pathways, gene expression, and chemosensitivity in human head and neck squamous cell carcinoma cell lines. Clin Cancer Res 2001;7:4220–9.
17. Ding Y, Sun X, Chen Y, Deng Y, Qian K. Epigallocatechin gallate attenuated non-alcoholic steatohepatitis induced by methionine- and choline-deficient diet. Eur J Pharmacol 2015;761:405–12.
18. Fuchs BC, Hoshida Y, Fujii T, Wei L, Yamada S, Lauwers GY, et al. Epidermal growth factor receptor inhibition attenuates liver fibrosis and development of hepatocellular carcinoma. Hepatology 2014;59:1577–90.
19. Lally JSV, Ghoshal S, DePeralta DK, Moaven O, Wei L, Masia R, et al. Inhibition of acetyl-CoA carboxylase by phosphorylation or the inhibitor ND-654 suppresses lipogenesis and hepatocellular carcinoma. Cell Metab 2019;29:174–82.
20. DePeralta DK, Wei L, Ghoshal S, Schmidt B, Lauwers GY, Lanuti M, et al. Metformin prevents hepatocellular carcinoma development by suppressing hepatic progenitor cell activation in a rat model of cirrhosis. Cancer 2016;122:1216–27.
21. Tolba R, Kraus T, Liedtke C, Schwarz M, Weiskirchen R. Diethylnitrosamine (DEN)-induced carcinogenic liver injury in mice. Lab Anim 2015;49:59–69.
22. Lee JS, Chu IS, Mikaelyan A, Calvisi DF, Heo J, Reddy JK, et al. Application of comparative functional genomics to identify best-fit mouse models to study human cancer. Nat Genet 2004;36:1306–11.

23. Dimri GP, Lee X, Basile G, Acosta M, Scott G, Roskelley C, et al. A biomarker that identifies senescent human cells in culture and in aging skin *in vivo*. Proc Natl Acad Sci U S A 1995;92:9363–7.
24. Hoshida Y, Villanueva A, Kobayashi M, Peix J, Chiang DY, Camargo A, et al. Gene expression in fixed tissues and outcome in hepatocellular carcinoma. N Engl J Med 2008;359:1995–2004.
25. Nakagawa S, Wei L, Song WM, Higashi T, Ghoshal S, Kim RS, et al. Molecular liver cancer prevention in cirrhosis by organ transcriptome analysis and lysophosphatidic acid pathway inhibition. Cancer Cell 2016;30:879–90.
26. Kurz DJ, Decary S, Hong Y, Erusalimsky JD. Senescence-associated (beta)-galactosidase reflects an increase in lysosomal mass during replicative ageing of human endothelial cells. J Cell Sci 2000;113: 3613–22.
27. Young AR, Narita M, Ferreira M, Kirschner K, Sadaie M, Darot JF, et al. Autophagy mediates the mitotic senescence transition. Genes Dev 2009;23:798–803.
28. Ahsan MK, Mehal WZ. Activation of adenosine receptor A2A increases HSC proliferation and inhibits death and senescence by down-regulation of p53 and Rb. Front Pharmacol 2014;5:69.
29. Hicks DF, Goossens N, Blas-García A, Tsuchida T, Wooden B, Wallace MC, et al. Transcriptome-based repurposing of apigenin as a potential anti-fibrotic agent targeting hepatic stellate cells. Sci Rep 2017;7:42563.
30. Zhang DY, Goossens N, Guo J, Tsai MC, Chou HI, Altunkaynak C, et al. A hepatic stellate cell gene expression signature associated with outcomes in hepatitis C cirrhosis and hepatocellular carcinoma after curative resection. Gut 2016;65:1754–64.
31. Krizhanovsky V, Yon M, Dickins RA, Hearn S, Simon J, Miething C, et al. Senescence of activated stellate cells limits liver fibrosis. Cell 2008; 134:657–67.
32. Xiao J, Ho CT, Liong EC, Nanji AA, Leung TM, Lau TY, et al. Epigallocatechin gallate attenuates fibrosis, oxidative stress, and inflammation in non-alcoholic fatty liver disease rat model through TGF/SMAD, PI3 K/Akt/FoxO1, and NF-kappa B pathways. Eur J Nutr 2014;53:187–99.
33. Shen K, Feng X, Su R, Xie H, Zhou L, Zheng S. Epigallocatechin 3-gallate ameliorates bile duct ligation induced liver injury in mice by modulation of mitochondrial oxidative stress and inflammation. PLoS One 2015;10:e0126278.
34. Tipoe GL, Leung TM, Liong EC, Lau TY, Fung ML, Nanji AA. Epigallocatechin-3-gallate (EGCG) reduces liver inflammation, oxidative stress and fibrosis in carbon tetrachloride (CCl4)-induced liver injury in mice. Toxicology 2010;273:45–52.
35. Chung MY, Park HJ, Manautou JE, Koo SI, Bruno RS. Green tea extract protects against nonalcoholic steatohepatitis in ob/ob mice by decreasing oxidative and nitrative stress responses induced by proinflammatory enzymes. J Nutr Biochem 2012;23:361–7.
36. Lambert JD, Kennett MJ, Sang S, Reuhl KR, Ju J, Yang CS. Hepatotoxicity of high oral dose (-)-epigallocatechin-3-gallate in mice. Food Chem Toxicol 2010;48:409–16.
37. Navarro VJ, Bonkovsky HL, Hwang SI, Vega M, Barnhart H, Serrano J. Catechins in dietary supplements and hepatotoxicity. Dig Dis Sci 2013; 58:2682–90.
38. Ullmann U, Haller J, Decourt JP, Girault N, Girault J, Richard-Caudron AS, et al. A single ascending dose study of epigallocatechin gallate in healthy volunteers. J Int Med Res 2003;31:88–101.
39. Yu Z, Samavat H, Dostal AM, Wang R, Torkelson CJ, Yang CS, et al. Effect of green tea supplements on liver enzyme elevation: results from a randomized intervention study in the United States. Cancer Prev Res 2017;10:571–9.
40. Ghany MG, Kleiner DE, Alter H, Doo E, Khokar F, Promrat K, et al. Progression of fibrosis in chronic hepatitis C. Gastroenterology 2003; 124:97–104.
41. Ramakrishna G, Rastogi A, Trehanpati N, Sen B, Khosla R, Sarin SK. From cirrhosis to hepatocellular carcinoma: new molecular insights on inflammation and cellular senescence. Liver Cancer 2013;2:367–83.
42. Singal AG, El-Serag HB. Hepatocellular carcinoma from epidemiology to prevention: translating knowledge into practice. Clin Gastroenterol Hepatol 2015;13:2140–51.
43. Park LS, Tate JP, Justice AC, Lo Re V III, Lim JK, Bräu N, et al. FIB-4 index is associated with hepatocellular carcinoma risk in HIV-infected patients. Cancer Epidemiol Biomarkers Prev 2011;20:2512–7.
44. Higashi T, Friedman SL, Hoshida Y. Hepatic stellate cells as key target in liver fibrosis. Adv Drug Deliv Rev 2017;121:27–42.
45. Jun JI, Lau LF. The matricellular protein CCN1 induces fibroblast senescence and restricts fibrosis in cutaneous wound healing. Nat Cell Biol 2010;12:676–85.
46. Li S, Ghoshal S, Sojoodi M, Arora G, Masia R, Erstad DJ, et al. Pioglitazone reduces hepatocellular carcinoma development in two rodent models of cirrhosis. J Gastrointest Surg 2019;23:101–11.
47. Gasser S, Orsulic S, Brown EJ, Raulet DH. The DNA damage pathway regulates innate immune system ligands of the NKG2D receptor. Nature 2005;436:1186–90.
48. Yoshimoto S, Loo TM, Atarashi K, Kanda H, Sato S, Oyadomari S, et al. Obesity-induced gut microbial metabolite promotes liver cancer through senescence secretome. Nature 2013;499:97–101.
49. Dapito DH, Mencin A, Gwak GY, Pradere JP, Jang MK, Mederacke I, et al. Promotion of hepatocellular carcinoma by the intestinal microbiota and TLR4. Cancer Cell 2012;21:504–16.
50. Lujambio A, Villanueva A. The usual SASPects of liver cancer. Aging 2015;7:348–9.
51. Coia H, Ma N, Hou Y, Dyba MD, Fu Y, Cruz MI, et al. Prevention of lipid peroxidation-derived cyclic DNA adduct and mutation in high-fat diet-induced hepatocarcinogenesis by Theaphenon E. Cancer Prev Res 2018;11:665–76.
52. Fu Y, Silverstein S, McCutcheon JN, Dyba M, Nath RG, Aggarwal M, et al. An endogenous DNA adduct as a prognostic biomarker for hepatocarcinogenesis and its prevention by Theaphenon E in mice. Hepatology 2018;67:159–70.
53. Inoue M, Kurahashi N, Iwasaki M, Shimazu T, Tanaka Y, Mizokami M, et al. Effect of coffee and green tea consumption on the risk of liver cancer: cohort analysis by hepatitis virus infection status. Cancer Epidemiol Biomarkers Prev 2009;18:1746–53.
54. Huang YQ, Lu X, Min H, Wu QQ, Shi XT, Bian KQ, et al. Green tea and liver cancer risk: a meta-analysis of prospective cohort studies in Asian populations. Nutrition 2016;32:3–8.
55. Ni CX, Gong H, Liu Y, Qi Y, Jiang CL, Zhang JP. Green tea consumption and the risk of liver cancer: a meta-analysis. Nutr Cancer 2017;69:211–20.
56. Tamura T, Hishida A, Wakai K. Coffee consumption and liver cancer risk in Japan: a meta-analysis of six prospective cohort studies. Nagoya J Med Sci 2019;81:143–50.